29

Hurricane-Induced Phytoplankton Blooms: Satellite Observations and Numerical Model Simulations

Menghua Wang[1], Xiaoming Liu[1,2], and Wei Shi[1,3]
[1]*NOAA National Environmental Satellite, Data, and Information Service Center for Satellite Applications and Research, Camp Springs, MD,*
[2]*SP Systems Inc., Greenbelt, MD,*
[3]*CIRA at Colorado State University, Fort Collins, CO, USA*

1. Introduction

Hurricane-force winds have significant effects on the upper ocean. Hurricane-induced vertical mixing, entrainment, and upwelling bring up cold and nutrient-rich sub-surface water to the surface. As a result, sea surface temperature (SST) cools several degrees Celsius as the mixed layer deepens by tens of meters, and conversely, downward mixing of heat also warms the upper seasonal thermocline waters. The nutrient-rich water in the upper euphotic zone can also stimulate biological production and phytoplankton bloom. The potential impact of hurricanes on upper ocean physics and biogeochemistry is quite complex, and their observation and study have benefited greatly from ocean satellite remote sensing. The Advanced Very High Resolution Radiometer (AVHRR) has been used for measuring SST for decades, and hurricane-induced SST drops have been reported (Price, 1981 and references therein). In comparison, the development of ocean color instruments onboard satellites observing ocean biological properties is relatively recent. With the advancement of satellite ocean color remote sensing from the Sea-viewing Wide Field-of-view Sensor (SeaWiFS) (Hooker *et al*., 1992) and the Moderate Resolution Imaging Spectroradiometer (MODIS) (Salomonson *et al*., 1989) in recent years, hurricane-induced phytoplankton blooms have been observed and reported (Babin *et al*., 2004; Lin *et al*., 2003; Miller *et al*., 2006; Walker *et al*., 2005; Shi and Wang, 2007).

The SeaWiFS, which has operated since August 1997, and MODIS on the Terra platform (December 1999–present) and Aqua platform (May 2002–present) have provided us a view of chlorophyll patterns and biospheres on global scales by using the advanced atmospheric correction algorithm for the data processing (Gordon, 1997; Gordon and Wang, 1994; IOCCG, 2010). For the global open oceans, both SeaWiFS and MODIS have been producing high-quality ocean color products (Bailey and Werdell, 2006; McClain *et al*., 2004), and these data have been used by researchers and scientists worldwide to study and understand the ocean's physical, optical, and biological changes and their effects on climate processes, as discussed in Behrenfeld *et al*. (2001), Chavez *et al*. (1999), and others.

However, in NASA's standard ocean color data processing system for MODIS, turbid waters caused by sediment mix-up and re-suspension may be misidentified as an enhanced chlorophyll-a (Chl-a) concentration and phytoplankton bloom due to very significant ocean contributions in near-infrared (NIR) wavelengths (Siegel *et al.*, 2000; Lavender *et al.*, 2005; Wang and Shi, 2005). To distinguish a phytoplankton bloom from hurricane-induced turbid waters, the shortwave infrared (SWIR) atmospheric correction algorithm (Wang and Shi, 2005; Wang, 2007; Wang *et al.*, 2009) is used to derive the normalized water-leaving radiance spectra from the blue to the NIR bands, as well as the Chl-a concentration following Hurricane Katrina (Shi and Wang, 2007). Compared with the NIR bands, waters are much strongly absorbing at the SWIR wavelengths (Hale and Querry, 1973). Thus, the black pixel assumption (i.e., zero ocean radiance contribution) at the SWIR wavelengths can be used for turbid and productive waters in deriving satellite ocean color products (Shi and Wang, 2009).

Satellite observations of SST and sea surface height (SSH) anomalies are also very useful for the investigation of hurricane impacts on upper ocean physical processes. Hurricanes are known to lower SST significantly during their passage, and this upper-ocean process depends on many factors such as mixed-layer depth, thermocline depth, air-sea heat fluxes, and the storm's intensity and transition speed. Despite its advantage of high spatial resolution, AVHRR SST measurement is available only in clear-sky conditions. On the other hand, Advanced Microwave Scanning Radiometer EOS (AMSR-E) on Aqua provides microwave-derived SST under both cloudy and clear-sky conditions, and is therefore very useful for continuous observations for periods before, during, and after hurricane passage. *Shi and Wang* (2007) used AMSR-E data to study the time series of SST in the Hurricane Katrina-induced phytoplankton bloom event in the Gulf of Mexico (GOM). SSH anomaly data derived from satellite altimetry measurements can provide mesoscale features like warm- or cold-core eddies in the ocean, which are sometimes not available in the SST measurement. Pre-existing mesoscale eddies on the hurricane track in the ocean have significant impacts on the upper ocean response to hurricanes. Since ocean eddies modulate the upper ocean's vertical and horizontal structures and heat balance, they are also very important in the oceanic response process to hurricanes. When a hurricane enters the warm (cold) core eddy, SST cooling may be greatly suppressed (intensified) due primarily to deep (shallow) mixed-layer and thermocline depth.

The GOM is greatly influenced by its unique ocean circulation feature, i.e., the Loop Current (LC). Warm water from the Caribbean Sea enters the Gulf of Mexico through the Yucatan Straits and then forms the LC. The LC penetrates northward into the Gulf of Mexico and then turns anti-cyclonically to flow southward along the steep west Florida shelf before turning eastward into the southern Straits of Florida (SSF). The Straits of Florida forms a conduit for the Florida Current (FC), which connects the LC with the Gulf Stream in the North Atlantic. The instability processes that are associated with LC shed warm core eddies (WCEs), which propagate westward and eventually dissipate along the shelf break. Cyclonic, cold-core eddies (CCEs), called Loop Current Frontal Eddies (LCFEs), are also formed along the shoreward boundary of the LC (Paluszkiewicz *et al.*, 1983; Vukovich, 1988; Fratantoni *et al.*, 1998; Romanou *et al.*, 2004). LCFEs travel rapidly southward downstream with the LC at speeds of 20–50 cm/s. Since the pre-existing oceanic features such as LC, WCE, and CCE can modulate the upper ocean vertical and horizontal structures and heat balance, they are also very important in the oceanic response process to hurricanes. When a hurricane enters the warm (cold) core eddy, SST cooling may be greatly suppressed (intensified) due primarily to deep (shallow) mixed-layer and thermocline depth. Using the

sea surface height (SSH) anomaly data derived from satellite altimetry measurements, *Liu et al.* (2009) reported that the Hurricane Katrina-induced phytoplankton bloom was coincident with a cyclonic eddy near the Dry Tortugas, and the pre-existing eddy played an important role in the phytoplankton bloom event.

Numerical simulation is an important approach to studying the upper ocean response to hurricanes. With a three-dimensional numerical model, the variations of ocean surface properties, such as SST and SSH, can be projected to water columns below the surface. *Price* (1981 and 1994) used a three-dimensional, primitive-equation, hydrostatic model that represents ocean upper mixed-layer and vertical structure on a fixed grid to simulate the physical processes of the hurricane-induced upwelling and mixing. *Liu et al.* (2009) used the Hybrid Coordinate Ocean Model (HYCOM) (Chassignet *et al*., 2003; 2007) to study the effect of the pre-existing eddy in the Hurricane Katrina-induced phytoplankton bloom in the GOM in 2005. HYCOM is a primitive-equation, ocean general circulation model that was evolved from the Miami Isopycnic-Coordinate Ocean Model (MICOM) (Bleck *et al*., 1992). In the study, the upper layer heat budget of the physical process was analyzed, and the nutrient enhancement in the upper layer was also simulated.

2. Upper-ocean physical response to hurricanes

Early observations of upper-ocean response to hurricanes have been reported and studied by *Leipper* (1967), *Brooks* (1983), *Sanford et al*. (1987), *Shay and Elsberry* (1987), *Shay et al*. (1989; 1998), *Brink* (1989), *Dickey et al*. (1998), and *Jacob et al*. (2000). *Price* (1981) summarized early hydrographic surveys and found two prominent features of the SST response to hurricanes: (1) hurricane-induced SST cooling increases as a hurricane's moving speed decreases and intensity increases; and (2) the SST response is markedly asymmetrical about the hurricane track. Hurricane-force winds (speeds greater than 33 m s^{-1}) have dramatic effects on the upper ocean. Frequently, near-surface waters cool several degrees Celsius as the mixed layer deepens by tens of meters with the most intense changes occurring under the more intense winds on the right-hand side (left-hand side in the Southern Hemisphere) of the storm track (Hazelworth, 1968; Dickey and Simpson, 1983; Stramma *et al*., 1986; Sanford *et al*., 1987). Conversely, downward mixing of heat causes the upper seasonal thermocline waters to warm. High-amplitude, near-inertial internal gravity waves (with vertical displacements of isotherms of a few tens of meters) and currents (around 1 m s^{-1}) are induced, which persist for several days, and geostrophic flows may also be produced (Shay and Elsberry, 1987; Shay *et al*., 1989, 1998; Dickey *et al*., 1998b; Zedler *et al*., 2002). The SST decrease is a result of both enhanced vertical mixing and upwelling induced by a near-inertial response of the oceanic mixed-layer to the asymmetric surface wind stress (Price, 1981; Shay and Elsberry, 1987), as well as flux-induced cooling.

The upper ocean response to a particular hurricane depends on several parameters involving atmospheric and oceanic variables (e.g., Price, 1981; Dickey *et al*., 1998b). Some of the important atmospheric variables include hurricane size (e.g., radius of tropical storm force winds, radius of hurricane-force winds), strength (wind speed), and transit speed. Intense, slowly moving hurricanes (~4 m s^{-1}) cause the most significant upwelling and the largest SST response (Price, 1981). Local hydrodynamic conditions, i.e., pre-existing stratification and near-inertial currents, also play an important role in the oceanic response to a hurricane, while the vertical distributions of nutrients and phytoplankton are primary factors in defining the resulting biogeochemical response.

Brink (1989) collected current data at depths from 159 to 1059 m at a location on the path of Hurricane Gloria in 1985 in the western North Atlantic and characterized the response of the deep thermocline and the downward propagation of near-inertial energy. *Dickey et al*. (1998) studied the Bermuda testbed mooring data during the passage of Hurricane Felix in August 1995. It was found that as Hurricane Felix passed the mooring, large inertial currents were generated within the upper layer by the onset of intense localized wind stress and lasted a period of approximately 22.8 hours. The current shear was the greatest at the base of the mixed layer, where deep cooler waters were entrained into the mixed layer resulting in cooling of the surface layer. The mixed-layer depth was about 15 m prior to the arrival of Felix, and deepened to about 45 m within three days after Felix's passage, according to the mooring. The temperature at 25 m decreased by 3.5–4.0°C and the temperature at 45 m increased by about 2.0°C through the mixing process. Temperatures at 71 m and greater depths decreased slightly.

Three-dimensional ocean numerical models were also used to study the physical process (Price, 1981; Price *et al*., 1994; Prasad and Hogan; 2007). *Price et al*. (1994) used a three-dimensional model to simulate ocean response to a moving hurricane and found that the ocean's response to hurricanes can be divided into two stages: forced and relaxation. In the forced stage, hurricane-force winds drive the mixed-layer currents, SST cooling by vertical mixing (entrainment), and air-sea heat exchanges (mainly due to loss of latent heat flux). The barotropic response consists of a geostrophic current and an associated trough in sea surface height. The relaxation stage response following a hurricane's passage is primarily due to inertial-gravity oscillations excited by the storm. The mixed-layer velocity oscillates with a near-inertial period, as do the divergence and associated upwelling and downwelling.

Entrainment has been emphasized as the dominant term in lowering the SST beneath a moving hurricane. Based on observations, *Jacob et al*. (2000) suggested that entrainment at the mixed-layer base generally accounts for ~75% to 90% of the cooling, while the *Price* (1981) model indicated that ~85% of heat flux into the mixed layer was through entrainment. Only about 10% to 15% of the cooling in the upper ocean is due to surface heat fluxes, which would range between 2000 and 3000 W m^{-2}. Estimations from *Jacob and Shay* (2003) ranged from ~10% to ~30% in the directly forced region. Horizontal advection is also found to be important in the mixed-layer heat balance during and subsequent to the passage of hurricanes (Price, 1981; Jacob *et al*., 2000). This contribution is particularly significant in the eddy region, where maximum cooling due to geostrophic advection (-0.69 °C d^{-1}) was as large as the surface heat flux term in the overall heat budget (Jacob *et al*., 2000).

3. Satellite observations of hurricane-induced phytoplankton blooms

With the advancement of satellite ocean color remote sensing from SeaWiFS and MODIS, hurricane-induced phytoplankton blooms were also observed and reported in the past decade (Babin *et al*., 2004; Lin *et al*., 2003; Miller *et al*., 2006; Walker *et al*., 2005). Hurricane-induced mixing, entrainment, and upwelling result in an increase in near-surface phytoplankton because phytoplankton is brought closer to the surface so that their photosynthetic system receives greater solar irradiance (Babin *et al*., 2004) and also because requisite nutrients are transported into the euphotic zone. On the other hand, the change of the phytoplankton in the ocean may lead to a time-lagged response of the colored dissolved organic matter (CDOM) (Hu *et al*., 2006). Enhanced CDOM induced by the storm in the

upper ocean layer has also been reported (Hoge and Lyon, 2002). In coastal regions, however, entrainment and upwelling can also result in sediment re-suspension and transport from nearby locations (Acker *et al*., 2002; Wren and Leonard, 2005). *Hu and Muller-Karger* (2007) also reported the hurricane-induced sediment re-suspension in the eastern Gulf of Mexico. To distinguish the phytoplankton bloom from turbid waters resulting from hurricane-induced sediment re-suspension and transportation, *Shi and Wang* (2007) used the SWIR atmospheric correction algorithm to derive the Chl-a concentration as well as the spectral normalized water-leaving radiance from the blue to the NIR bands. The normalized water-leaving radiance spectra were also used to discriminate the phytoplankton bloom from the storm-induced CDOM.

Babin et al. (2004) examined the passages of 13 hurricanes through the Sargasso Sea region of the North Atlantic during the years of 1998 through 2001, and the remotely sensed chlorophyll-a data from SeaWiFS were used to analyze the hurricane-induced phytoplankton blooms. The SeaWiFS data shows increased concentrations of surface chlorophyll within the cool wakes of the hurricanes, apparently in response to the injection of nutrients and/or biogenic pigments into the oligotrophic surface waters. The observed increases in Chl-a in the wakes of these hurricanes ranged from a minimum of ~5% to a maximum of ~91%. This maximum is comparable to the spring bloom near Bermuda, which shows an increase of over 100% but with absolute magnitudes more pronounced than our observations of hurricane wakes. This increase in post-storm surface chlorophyll-a concentration usually lasted about two to three weeks before it returned to its nominal pre-hurricane level.

Lin et al. (2003) presented evidence of the Tropical Cyclone Kai-Tak-induced phytoplankton bloom in the South China Sea (SCS) in July 2000. During its short three-day stay, Kai-Tak triggered an average 30-fold increase in surface chlorophyll-a concentration. The estimated carbon fixation resulting from this event alone is 0.8 Mt, or ~2–4% of SCS's annual new production. Given an average of ~14 cyclones passing over the SCS annually, it was suggested that the long-neglected contribution of tropical cyclones to SCS's annual new production may be as much as ~20–30%. In addition, *Walker et al*. (2005) analyzed the remotely sensed SST and Chl-a data subsequent to Hurricane Ivan's passage across the Gulf of Mexico in September 2004, and revealed sea surface cooling of 3–7°C and elevated Chl-a concentrations over two large areas along Ivan's track. Within the northern area of cooling, concentrations increased from 0.36 mg/m^3 (before Ivan) to 0.81 mg/m^3 (after Ivan) over a region of ~27,000 km^2. In the southern region, mean Chl-a concentrations increased from 0.24 mg/m^3 to 0.99 mg/m^3 over a region of ~13,000 km^2. Peak concentrations lagged Ivan's passage by 3 and 4 days in the northern and southern features, respectively. *Walker et al*. (2005) also reported that the increases of hurricane-forced upwelling and chlorophyll-a concentrations could be enhanced within cold-core cyclones in the Gulf of Mexico.

4. Hurricane Katrina-Induced phytoplankton bloom

Shi and Wang (2007) reported a Hurricane Katrina-induced SST cooling and a phytoplankton bloom in the Gulf of Mexico in August 2005. In their study, combined data sets of sea surface wind from the National Center for Environmental Prediction (NCEP), SST from AMSR-E, and ocean color products from MODIS-Aqua are used to analyze physical, optical, and biological processes after Hurricane Katrina. MODIS-Aqua data were processed using the SWIR atmospheric correction algorithm (Wang, 2007; Wang and Shi, 2005). It has been

demonstrated that, compared to using the NASA standard algorithm (Gordon and Wang, 1994), use of the SWIR algorithm ocean color products can be improved over productive ocean waters (Wang *et al*., 2007; 2009). Therefore, the phytoplankton bloom can be distinguished from sediment re-suspension and transportation, which can also be induced by a hurricane in coastal waters. The AMSR-E measurements produce the microwave SST under both cloudy and clear sky conditions (Wentz *et al*., 2000). Therefore, AMSR-E data are quite useful for continuous observations of the SST for the periods before, during, and after hurricane passage.

Hurricane Katrina formed as a tropical depression over the southeastern Bahamas on August 23, 2005, and was then upgraded to tropical storm status on August 24. The tropical storm continued to move towards Florida, and became a hurricane near 2100 UTC on August 25, 2005, only two hours before it made landfall on the southeastern coast of Florida. The storm weakened over land, but it regained hurricane status about one hour after entering the Gulf of Mexico. The storm rapidly intensified after entering the Gulf because of the storm's movement over the LC warm waters. On August 27, the storm reached Category 3 intensity, becoming the third major hurricane of the season. Katrina again rapidly intensified, attaining Category 5 status on August 28. The pressure measurement made Katrina the fourth most intense Atlantic hurricane on record, and it was also the strongest hurricane ever recorded in the Gulf of Mexico at the time. Katrina made its second landfall on August 29 as a Category 3 hurricane with sustained winds of 125 mph (205 km/h) near Buras-Triumph, Louisiana.

Shi and Wang (2007) analyzed Hurricane Katrina wind fields from NCEP and estimated the upwelling speed induced by the wind stress curl. The track of Hurricane Katrina is outlined in red as shown in Figure 1 (Shi and Wang, 2007), and the hurricane eye location is marked by a red square at 6-hour intervals. Also shown in Fig. 1 is a snapshot of the Katrina wind field at 0600 UTC, August 27th from NCEP, when the hurricane eye was located at a latitude and longitude of (24.4°N, 84.0°W), and the maximum sustained wind speed reached ~30 m/s. At this location, Hurricane Katrina was also found moving slowly with a speed of ~3 m/s, about a half of the moving speed before landing in New Orleans. The wind stress curl-induced ocean upwelling was calculated by *Shi and Wang* (2007) as shown in Fig. 2. The highest upwelling velocity is estimated to be ~2.0×10^{-3} m/s, and the strongest upwelling is located almost in the hurricane center.

A notable phytoplankton bloom centered at a location of (24°N, 84°W) was observed four days after Katrina's passage (Shi and Wang, 2007). Before Katrina, Chl-a concentration was low at ~0.1-0.2 mg/m^3 for the whole Gulf region. Two days after the passage of Hurricane Katrina, enhanced Chl-a concentration can be observed in the large regions east of the Gulf of Mexico. A notable patch of high Chl-a concentration with value ~1.5 mg/m3 was observed. The elevated Chl-a region coincides with the location of the hurricane eye and the area with a strong upwelling. On September 7, while the patch of phytoplankton bloom can still be observed, Chl-a magnitude decreased significantly with values at ~0.2 to 0.3 mg/m^3. Basin-wide, the Chl-a concentration level dropped back to the pre-Katrina level.

Figure 3 provides, quantitatively, the time series of the wind speed, SST, and Chl-a concentration at the center of the bloom located at (24.19°N, 84.06°W). Due to frequent cloud coverage, only nine Chl-a data were obtained. Obviously, the ocean physical response (SST) and the biological response (Chl-a) lag the hurricane winds. Before Katrina, SST at this location was ~31°C and Chl-a concentration ~0.1 mg/m^3. The wind speed started to pick up on August 25, and reached the maximum on August 27. However, there was no substantial

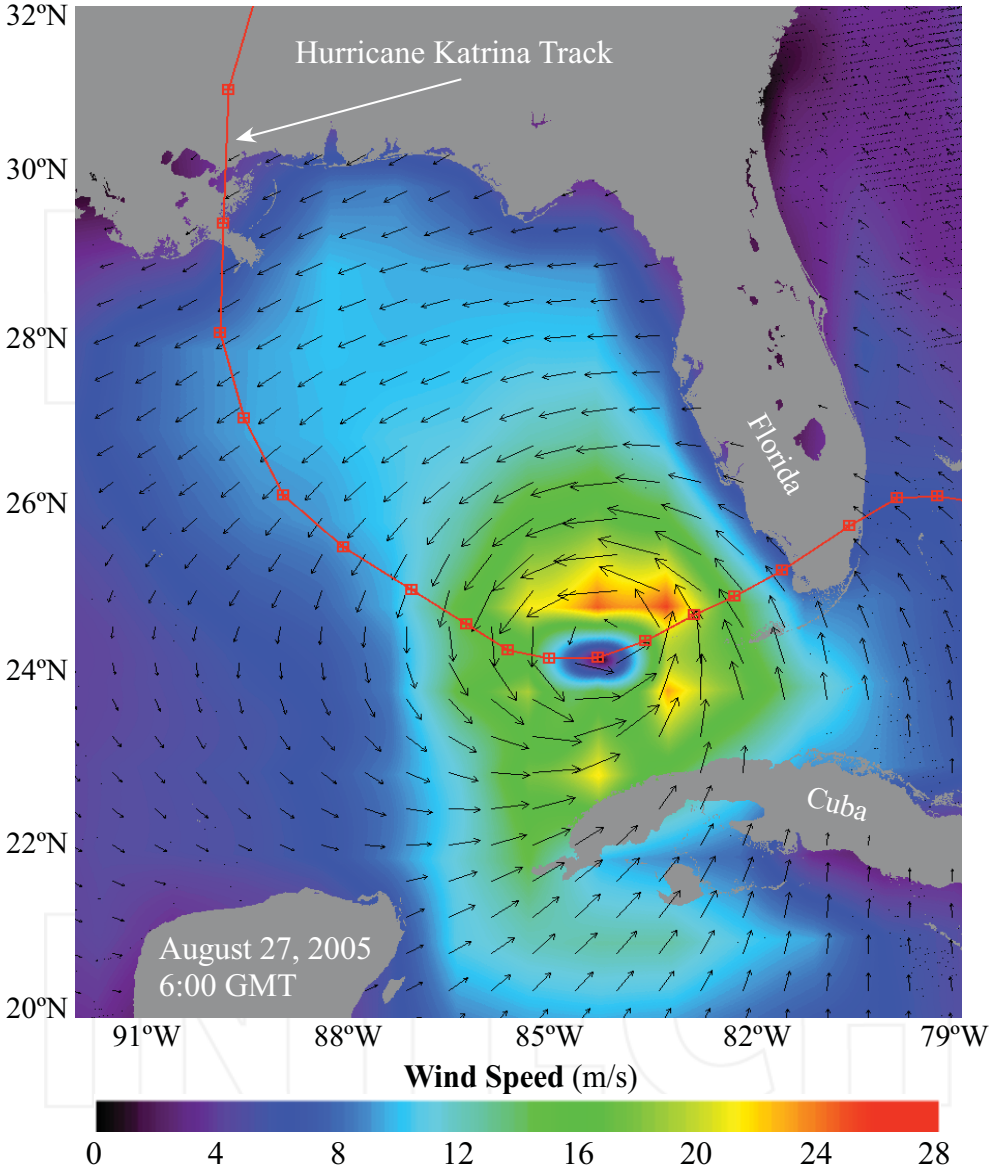

Fig. 1. Snapshot of Hurricane Katrina wind fields at 0600 UTC, August 27, 2005, with the track of the hurricane outlined in red (reproduced from *Shi and Wang* (2007)). The hurricane eye location is marked by red squares at intervals of every 6 hours.

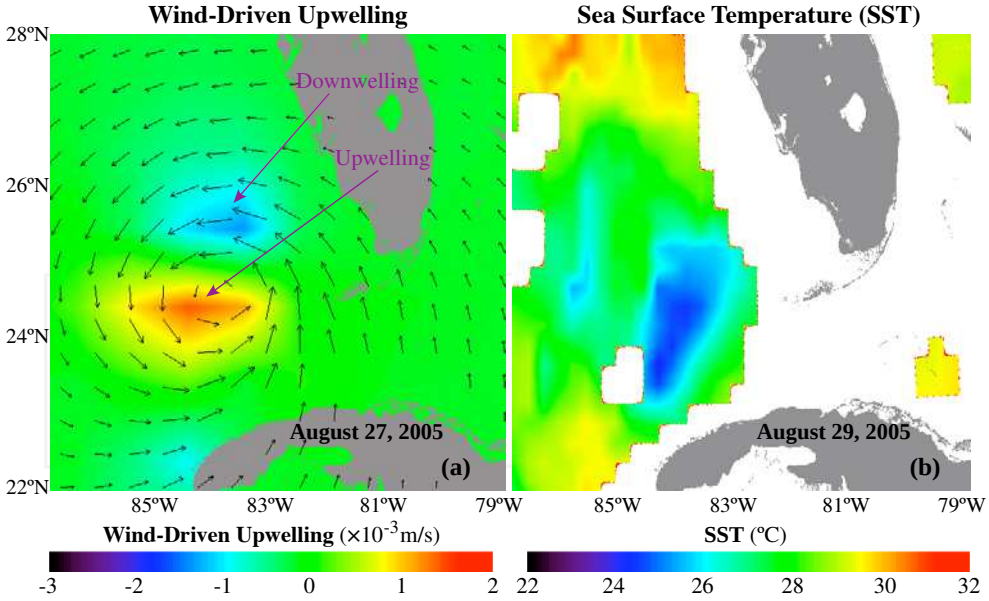

Fig. 2. Hurricane Katrina-induced ocean physical responses as presented in images of (a) the wind-driven upwelling on August 27, 2005 and (b) the microwave SST on August 29, 2005 (reproduced from *Shi and Wang* (2007)).

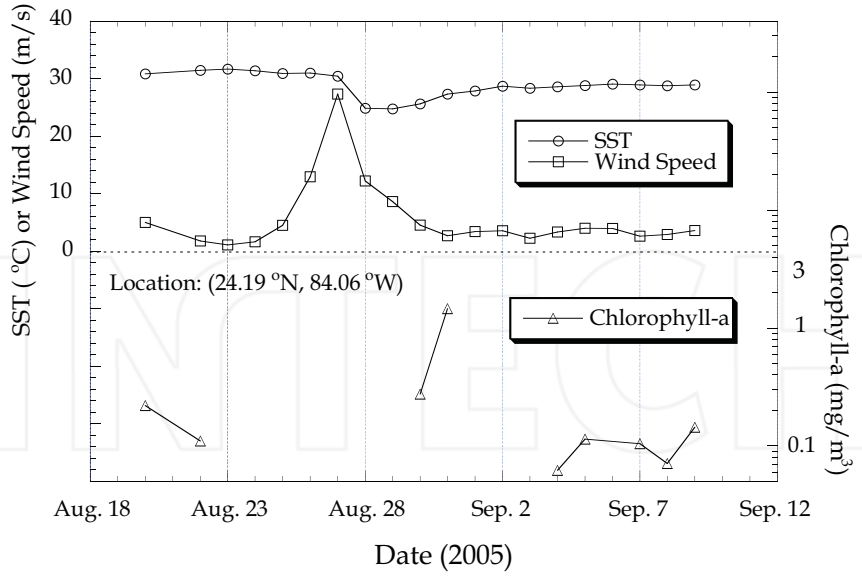

Fig. 3. The time series of the wind speed, SST, and Chl-a concentration at the center of the bloom located at (24.19˚N, 84.06˚W) from August 20 to September 9, 2005 (reproduced from *Shi and Wang* (2007)).

SST drop during this period. The SST at this location reached the lowest level on August 28, one day after the hurricane passed. Unfortunately, there was no ocean color data available during the hurricane period. The phytoplankton bloom can be seen picking up slightly on August 30 with Chl-a concentration of ~0.3 mg/m^3 from the pre-Katrina value of ~0.1 mg/m^3. It reached ~1.5 mg/m^3 on the next day, August 31. One week later on September 7, SST gradually increased to ~29°C, but still below the pre-Katrina SST. The phytoplankton bloom also decayed quickly, and Chl-a values returned to pre-Katrina levels as early as September 4.

Nutrients such as nitrate and phosphate are critical to phytoplankton growth in the ocean. *Shi and Wang* (2007) analyzed the water temperature and nutrient fields from the climatology data set (Levitus *et al*., 1994), and found from the after-Katrina SST value that the waters were between a depth of ~80 and 100 m at the phytoplankton bloom location. At that depth, the nitrate and phosphate concentrations are nearly four to five times higher than that at the surface values, according to the climatology data (Levitus *et al*., 1994). Following strong upwelling and vertical entrainment mixing, however, nutrient concentration could be elevated on the surface and provide the required nutrient supply for the phytoplankton bloom. It was concluded that the phytoplankton bloom was triggered by abnormally high nutrient concentrations due to a strong entrainment mixing and upwelling following the passage of Hurricane Katrina.

5. Numerical simulation of hurricane Katrina-induced phytoplankton bloom

Liu et al. (2009) presented some further evidence from SSH anomaly data derived from satellite altimetry measurements obtained from the Colorado Center for Astrodynamics Research (CCAR) at the University of Colorado, which shows that the Hurricane Katrina-induced phytoplankton bloom near (24°N, 84°W) was coincident with a cyclonic eddy near the Dry Tortugas (Fig. 4). These observations indicate that the cyclonic eddy might have played a critical role in the phytoplankton bloom event. Near the Dry Tortugas, the Tortugas gyre often occurs when the southward flowing LC overshoots entry into the Straits of Florida and approaches the coast of Cuba before abruptly turning to the east (Lee *et al*., 1992; 1995). This offshore position of the Florida Current, combined with the strong cyclonic curvature of the flow field, can cause a counterclockwise recirculation off the Tortugas, i.e., the "Tortugas gyre" (Lee *et al*., 1995). In a cyclonic eddy, the cold nutrient-rich waters from the deep layer stimulate primary production.

To further investigate the mechanism of the Katrina-induced phytoplankton bloom and the role of the pre-existing cyclonic eddy, *Liu et al*. (2009) simulated the process of the upper ocean response to Hurricane Katrina using the HYCOM model (Bleck, 2002). Particularly, two experiments with and without the presence of a pre-existing cyclone eddy near the Dry Tortugas were simulated and the results were compared. In addition to the standard physical parameters, such as temperature and salinity in HYCOM, three nutrient parameters—nitrate, phosphate, and silicate—were also included in the simulation to study the process of the Katrina-induced nutrient enhancement in the upper ocean.

To evaluate the importance of the cold-core eddy on the physical, chemical, and biological responses of the ocean to hurricane forcing, and to identify the mechanism of the hurricane-driven bloom, the north Atlantic HYCOM model configuration developed by *Xie et al*. (2007) was used to spin up the HYCOM model. Two cases with and without cold-core front eddy were then identified. The ocean conditions for these two cases were set up as the initial

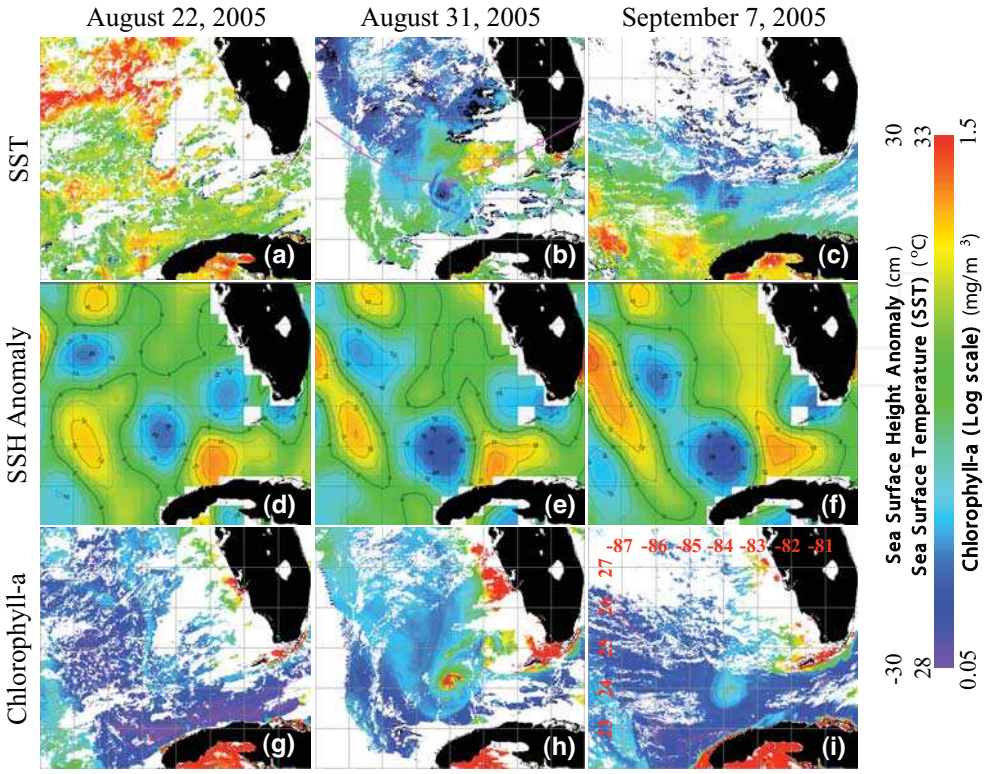

Fig. 4. Satellite-derived (a–c) MODIS SST, (d–f) SSH anomaly, and (g–i) MODIS chlorophyll-a concentration on August 22, August 31, and September 7, 2005, respectively. SSH anomaly data is from Center for Astrodynamics Research (CCAR). Plot (b) also shows the Hurricane Katrina eye locations (marked by a pink square) at 6-hour intervals. Latitude and longitude for the region are indicated in plot (i). Figure 4 was reproduced from *Liu et al.* (2009).

condition, and then wind forcing associated with Hurricane Katrina was applied to these two cases. The model domain covers the north and equatorial Atlantic (98°W–14°E, 17°S–52°N). The horizontal resolution is 0.18° and the vertical resolution is 22 layers that move vertically as a function of total depth. The model was spun up for one year with an initial condition constructed from the Levitus Data Set (Levitus, 1982) and forced by the Comprehensive Ocean Atmosphere Data Set's (COADS) monthly climatology atmospheric forcing including wind, air-temperature, relative humidity, and short-wave and long-wave radiations. The results were then used as the initial conditions of the hurricane response for simulations.

In the study, two cases of LC states near the Dry Tortugas on two different model days were chosen: Experiment I, with the presence of a cyclone eddy near (24°N, 84°W); and Experiment II, without the presence of a cyclone eddy near the Dry Tortugas. Since the differences between the mean monthly climatology of July and August in the vertical structure are small when compared with the differences between the two cases with and without the presence of the eddy, it was assumed that the differences in the simulations

between the two cases were mainly caused by the eddy. The annual mean fields of nitrate, phosphate, and silicate were extracted from the *World Ocean Atlas 2005* and set as the initial conditions of the nutrients at the beginning of both experiments. The two cases of hurricane simulations were carried out from August 25–31, 2005, and driven by the NCEP atmospheric forcing fields of wind, air-temperature, and relative humidity at the ocean surface.

Figure 5 shows the SST map near the LC before and after Hurricane Katrina's passage in Experiment I (Figs. 5a and 5b) and Experiment II (Figs. 5c and 5d). In both cases, the area was dominated by warm SSTs of ~30°C on August 27 before Hurricane Katrina (Figs. 5a and 5c). However, after Hurricane Katrina, the SST cooling shows quite large differences between the two cases: in Experiment I (Fig. 5b), the maximum SST drop (~4°C) is at the location of the cold-core eddy, and the SST cooling inside of the LC frontal eddy is much more significant than other areas; in Experiment II (Fig. 5d), SST cooling shows no significant difference in the observed phytoplankton bloom location than other areas on the hurricane track.

The time series of vertical temperature profile and mixed-layer depth near the location of the observed phytoplankton bloom (24°N, 84°W) in the two experiments are shown in Figure 6. Before Hurricane Katrina, the surface waters down to ~30 m depth were dominated by warm temperature >29°C in both cases. However, the vertical structure below

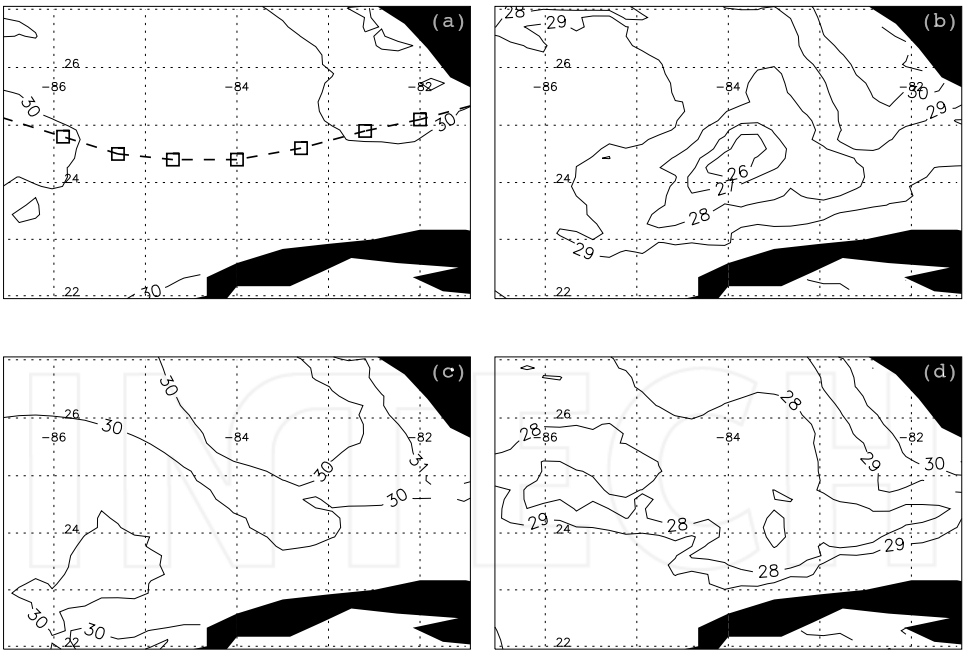

Fig. 5. Model simulated SST in (a–b) Experiment I and (c–d) Experiment II (units: °C). Plots (a) and (c) are on August 27, and plots (b) and (d) are on August 29, respectively. Katrina's track is overlaid in plot (a) as a dashed line with square symbols. Figure 5 was reproduced from *Liu et al.* (2009).

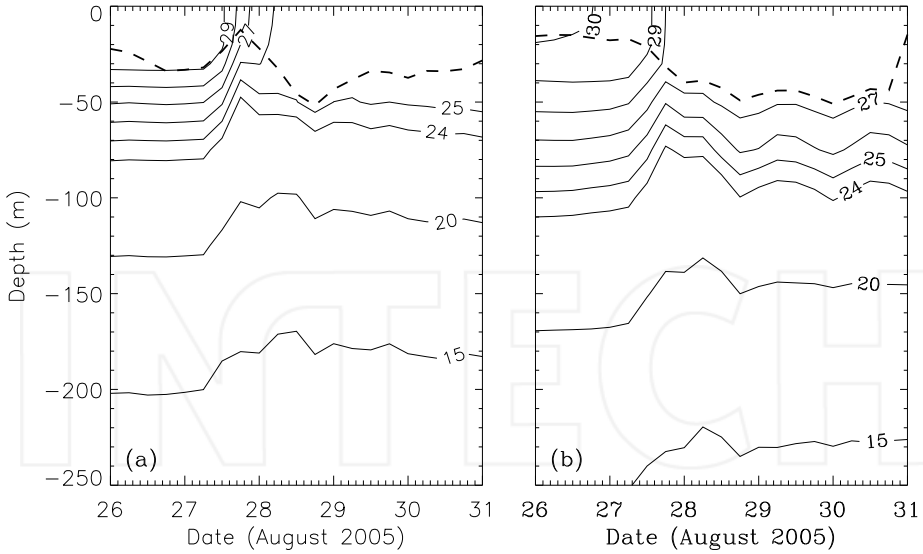

Fig. 6. Time series of vertical temperature profile at (24°N, 84°W) in (a) Experiment I and (b) Experiment II (units: °C). Mixed-layer depth is indicated as the dashed line (reproduced from *Liu et al.* (2009)).

the surface shows a large difference between the two cases due to different LC states. Without the presence of the cyclone eddy in Experiment II (Fig. 6b), the location of the observed phytoplankton bloom is on the path of the LC, and, thus, is dominated by warm LC waters. In this case, the isotherms are deep, e.g., the 26°C isotherm is at ~85 m depth. With the presence of the cyclone eddy in Experiment I (Fig. 6a), the isotherms are elevated, and the 26°C isotherm is now at ~60 m, which is 25 m shallower than in Experiment II. In Experiment I, strong hurricane-induced upwelling lifted up the isotherms by ~30 m on August 27, and the mixed-layer depth was also decreased. Due to strong vertical diffusion, the mixed-layer depth deepened by ~40 m on August 28, and then it started to decrease gradually. The maximum mixed-layer depth was about 50 m, and coldest temperature below the mixed-layer depth was 25°C, which was originally located at ~70 m depth before Katrina. Thus, the deepest layer that contributed to the surface cooling was at ~70 m depth. The significant mixed-layer temperature cooling occurred between August 27 and 28, which was similar to satellite SST observations. In Experiment II, because the location was under the influence of LC advection, changes of mixed-layer depth and vertical profiles were different from those in Experiment I. The upwelling and vertical diffusion processes were not as strong as in Experiment I, and the isotherms were deeper. The 27°C isotherm was well below the bottom of the mixed layer during and after Katrina's passage, never reaching the surface.

The initial surface nitrate, phosphate, and silicate concentrations were about 0.8μM, 0.1μM and 1.6μM, respectively, in both cases before Hurricane Katrina. The basic mechanism of nutrient response was the same as temperature: deep nutrient-rich waters were brought up to the surface by hurricane-induced strong upwelling and vertical diffusion processes during the Katrina passage. Figure 7 shows the post-Katrina/prior-Katrina ratio of surface

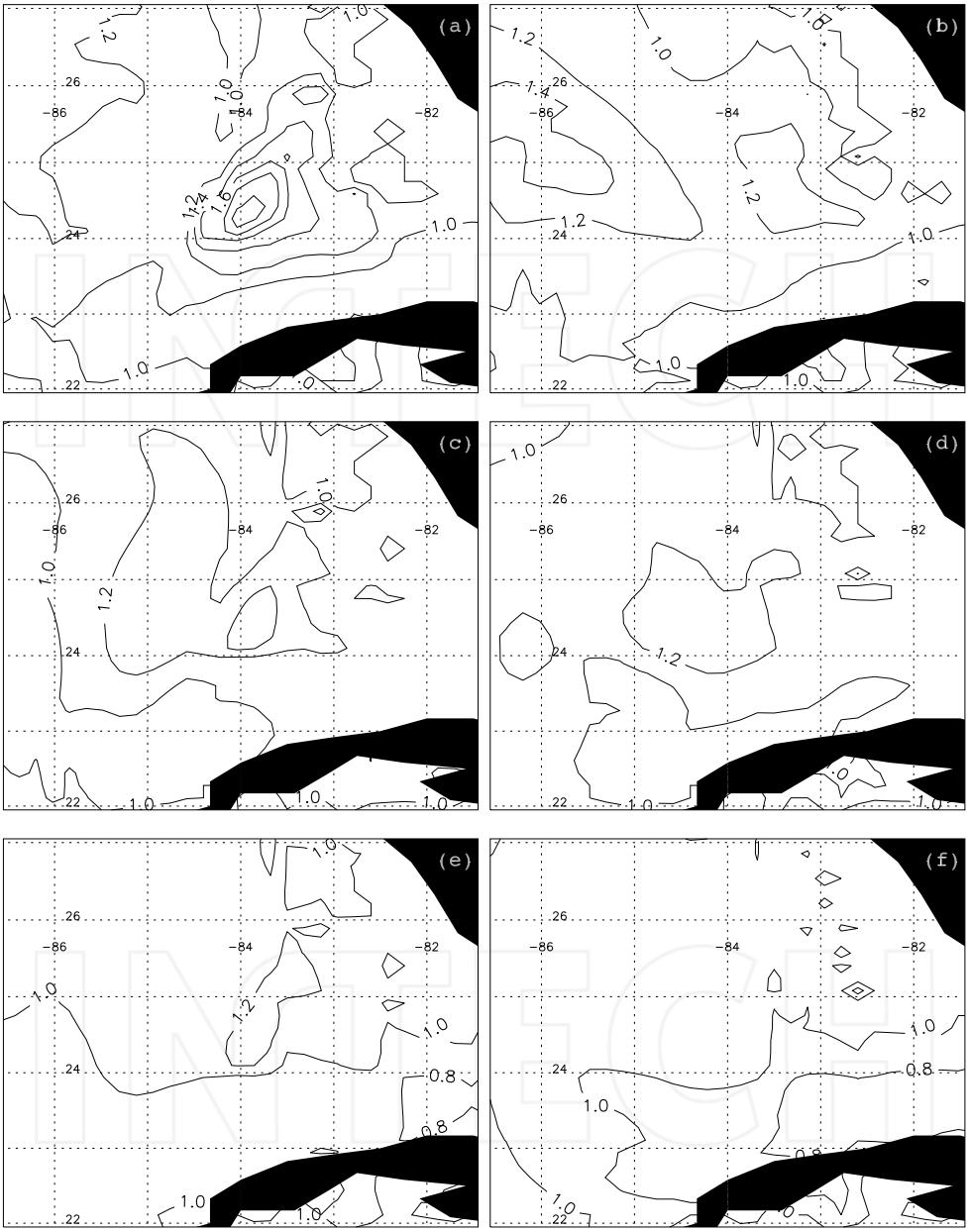

Fig. 7. Post-Katrina/prior Katrina ratio of (a–b) nitrate, (c–d) phosphate, and (e–f) silicate. Plots (a), (c) and (e) are from Experiment I, and plots (b), (d), and (f) are from Experiment II. Data from August 27 and August 29 are used as the prior-Katrina and post-Katrina data, respectively. Figure 7 was reproduced from *Liu et al.* (2009).

nitrate, phosphate, and silicate concentrations. In Experiment I, all three types of nutrient concentrations within the cyclone eddy increased more significantly than in other areas on the hurricane track. The maximum nutrient concentration increase occurred at the location of the observed phytoplankton bloom (24°N, 84°W). The nitrate concentration increased most significantly by ~100% at the location of the observed phytoplankton bloom, while phosphate and silicate concentration increased ~40% and ~20%, respectively. In Experiment II, nitrate, phosphate, and silicate concentrations at (24°N, 84°W) did not show more significant increases than in other areas on the hurricane track. In general, the enhancement of all three nutrient concentrations was less than 20%.

Figure 8 shows the time series of nitrate, phosphate, and silicate vertical profiles at (24°N, 84°W). Before Katrina, the subsurface nitrate concentrations in Experiment I were higher than in Experiment II at the same depth (Figs. 8a and 8b). For example, at a 70 m depth, the nitrate concentration was ~2.0 μM in Experiment I, while it was only ~1.2 μM in Experiment II. This was primarily due to cyclone eddy-induced upwelling, which elevated the nitrate levels in Experiment I. The differences in the initial vertical structure between the two cases consequently led to different results in the nitrate response to Katrina. In Experiment I, waters at a 70 m depth with a nitrate concentration of ~2.0 μM were lifted up by ~30 m and further entrained into the mixed layer, which significantly increased the nitrate concentrations at the surface. The surface nitrate concentration increased dramatically between August 27 and 28, and the increase was in phase with SST cooling as shown in Fig. 6a. In Experiment II, however, the 2.0 μM contour line is well below the bottom of the mixed-layer, and does not contribute to the surface nitrate enhancement. The maximum nitrate concentration at the mixed-layer base is about 1.2 μM, and thus the change of the nitrate concentration at the surface is less significant compared with Experiment I.

The phosphate vertical profile (Figs. 8c and 8d) shows a similar pattern to that of nitrate in the two experiments. In Experiment I, the surface phosphate concentration increased from ~0.1 μM to ~0.14 μM after Katrina passed near the location of the observed phytoplankton bloom. Before Katrina, the 0.14 μM contour line was originally at ~70 m depth, and it was uplifted and further entrained into the mixed layer during the Katrina passage. The 0.16 μM contour line, which was originally at ~80 m depth, never reached the surface. Therefore, the impact of the hurricane-induced upwelling and vertical diffusion can reach ~70 m depth, which was consistent with the results of nitrate concentration. In Experiment II, the contour lines are much deeper than in Experiment I. In this case, waters with 0.14 μM phosphate concentration were originally at 90 m depth and well below the bottom of the mixed layer during the Katrina passage. Before Katrina, the phosphate concentration at a 70 m depth was ~0.12 μM. Although it was brought up to the surface by the upwelling and vertical diffusion, it did not enhance the surface phosphate concentration due to little vertical gradient in the top 70 meters.

The surface silicate concentrations show much less significant changes after Katrina's passage compared with nitrate and phosphate (Figs. 8e and 8f). Before Katrina, although the silicate concentration was higher in Experiment I than at the same depth in Experiment II, it can be seen that in both cases, the vertical gradient of silicate concentration was minimal in the top 70 m depth. Consequently, the upwelling and vertical diffusion process does not significantly increase the surface silicate levels in either of the experiments.

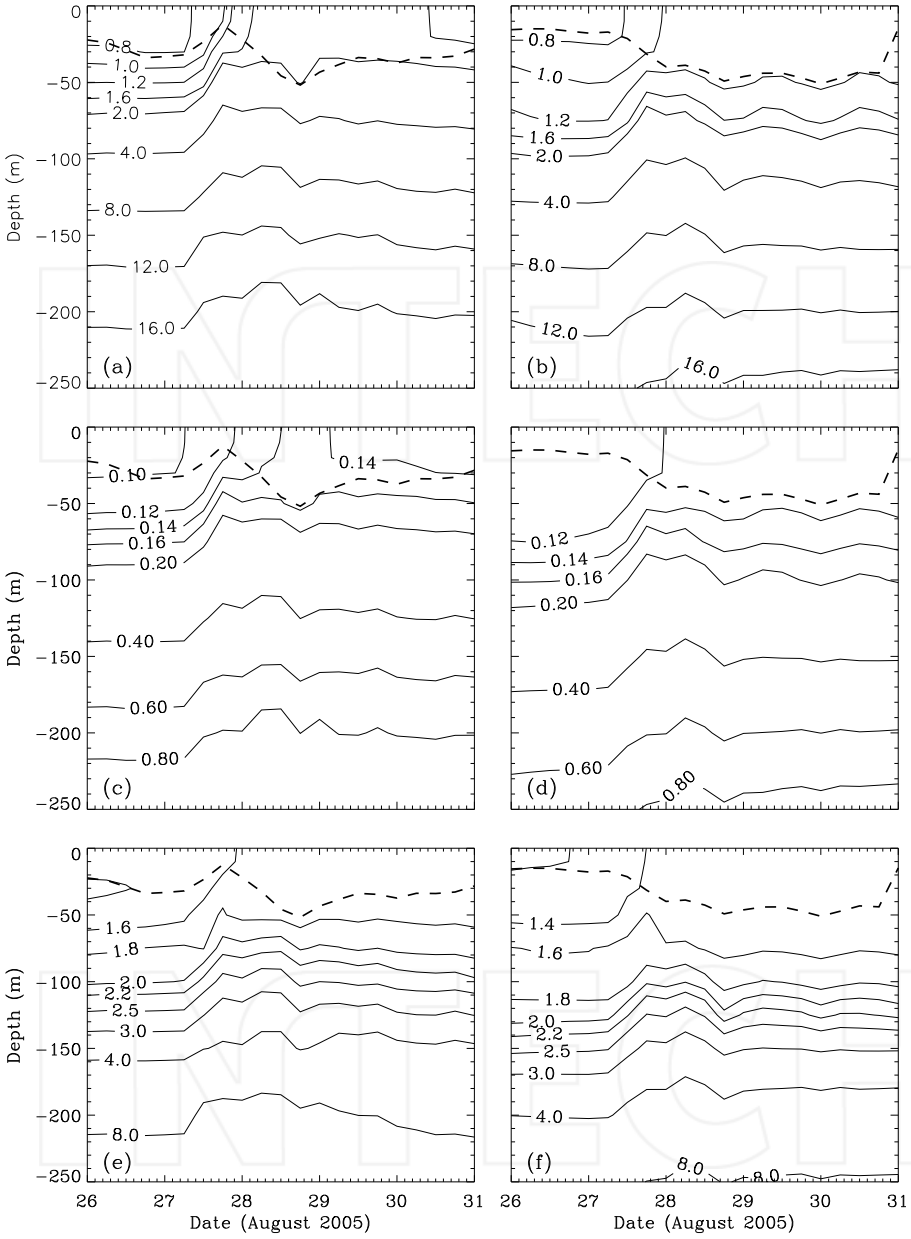

Fig. 8. Time series of vertical profile of (a–b) nitrate, (c–d) phosphate, and (e–f) silicate at (24°N, 84°W). Plots (a), (c), and (e) are from Experiment I, and plots (b), (d), and (f) are from Experiment II (units: μM). Mixed-layer depth is indicated as the dashed line. Figure 8 was reproduced from *Liu et al.* (2009).

6. Discussions and summary

In this chapter, we reviewed the status of research on the upper-ocean physical response to hurricanes and the hurricane-induced phytoplankton blooms observed by the satellite remote sensing. Using the phytoplankton bloom triggered by Hurricane Katrina as an example, a notable phytoplankton bloom triggered by hurricane wind-driven upwelling and vertical mixing is analyzed and quantified with combined data sets of the NCEP winds, AMSR-E microwave SST, and MODIS ocean color products. MODIS-Aqua ocean color observation shows that the hurricane-driven phytoplankton bloom lasted less than one week. By looking at both the blue and the NIR ocean contributions, we conclude that the phytoplankton bloom is the only source for the ocean surface optical property change after Hurricane Katrina. In addition, AMSR-E SST and MODIS-Aqua ocean color observations show that physical and biological responses to the hurricane are not synchronized with the hurricane winds. Indeed, it is found that the ocean physical response as represented by SST lags the hurricane peak wind speed by about one day, while the maximum biological response could be observed nearly four days later after the passing of the hurricane.

Indeed, satellite observations (e.g., AMSR-E and MODIS-Aqua) provide us with effective tools to monitor the physical, optical, geochemical, and biological changes of the ocean environments following an extreme weather event such as a hurricane. They also extend further evidence that the tropical cyclone is an important mechanism to pump nutrients into the upper euphotic zone and result in significant phytoplankton blooms, thereby leading to an increase of the ocean's primary production.

Even though satellite observations provide insights on the phytoplankton and its relationship with the physical response and nutrient supply changes following a hurricane, the location of the phytoplankton bloom at (24°N, 84°W) cannot be explained only by upwelling and vertical diffusion associated with Hurricane Katrina. In fact, it has been well documented that the maximum SST drop usually occurs to the right of the hurricane track because of the asymmetry in turning direction of the wind-stress vector that drives a very strong asymmetry in the mixed-layer velocity (Price, 1981). On the contrary, the observed Katrina-induced maximum SST drop and phytoplankton bloom at (24°N, 84°W) occurred on the left of the hurricane track. According to a National Hurricane Center report (www.nhc.noaa.gov/pdf/TCR-AL122005_katrina.pdf), the center of Hurricane Katrina was at (24.5°N, 84°W) while moving towards the west on August 27 at 0600 UTC. Thus, the location of the observed maximum SST drop and the center of the phytoplankton bloom is 20–30 km left on the hurricane track. The co-location of the cyclone eddy and the phytoplankton bloom explains this contradiction to the classic rightward-bias response theories: the pre-existing cold-core eddy at (24°N, 84°W) played an important role in the bloom event.

The numerical simulations in this study have further supported this hypothesis. The simulation results show that the SST cooling is more significant in the presence of the cyclone eddy at the location of the observed phytoplankton bloom. Although the response of the surface nitrate, phosphate, and silicate concentrations is due to the same mechanism of upwelling and vertical diffusion that induces SST cooling, the enhancement of the three types of nutrient concentrations at the surface are quite different. The surface nitrate and phosphate concentrations increase by ~100% and 40%, respectively, while the surface silicate concentration increase only ~20%. Given the same strength of upwelling and vertical diffusion, the enhancement of the surface nutrient levels depends on the initial vertical

gradient of the subsurface nutrient concentrations within the maximum depth that the upwelling and vertical diffusion processes can reach. Generally, the vertical gradient of the nitrate and phosphate concentrations within the top 70 m depth are larger than that of silicate, and thus lead to much more significant surface enhancement. In addition, the pre-existing cyclonic eddy greatly enhances the vertical gradient of nitrate and phosphate in the top 70 m depth, and consequently leads to more significant surface nitrate and phosphate concentrations in Experiment I. However, because of deep nutricline in the silicate vertical profile, the eddy does little enhancement on its vertical gradient of the top 70 m depth. Thus, there is little difference in the surface silicate enhancement between the two simulated cases.

Satellite observations revealed that Hurricane Katrina led to a significant SST cooling and a phytoplankton bloom near (24°N, 84°W) in the Gulf of Mexico. The SSH anomaly derived from satellite altimetry also showed that a southward-propagating Loop Current frontal eddy co-located with the phytoplankton bloom, which suggested that the eddy was an important factor in the phytoplankton bloom event. In this study, HYCOM is used to study the process of upper ocean responses to Hurricane Katrina. Two different cases with and without the presence of a cyclone eddy at the location of the observed phytoplankton bloom are simulated. The model run demonstrates that the Katrina-induced phytoplankton bloom is attributed to the pre-existing eddy, as well as to a slow-moving hurricane. The cyclonic eddy plays a critical role in the development of the Katrina-induced bloom, and it significantly strengthens the upper ocean dynamics and nutrient responses. In the simulations, the Katrina-induced upwelling and vertical diffusion process can reach ~70 m depth. The cyclonic eddy in the phytoplankton bloom area uplifted the isotherms and increased vertical temperature, nitrate, and phosphate gradients in the upper 70 m depth, thus leading to more significant SST cooling and increases in nitrate and phosphate concentrations than in the non-eddy case. Our model results also suggest that the nitrate concentration plays a dominant role in the development of the phytoplankton bloom with over 100% increase in the surface concentration, while the phosphate increases ~40%. The silicate has a minimal effect on the bloom with the smallest increase for its surface concentration.

7. Acknowledgments

The views, opinions, and findings contained in this article are those of the authors and should not be construed as an official NOAA or U.S. Government position, policy, or decision.

8. References

Acker, J. G., C. W. Brown, A. C. Hine, E. Armstrong, and N. Kuring (2002), Satellite remote sensing observations and serial photography of storm-induced neritic carbonate transport from shallow carbonate platforms, *Int. J. Remote Sens*., 23, 2853– 2868.

Babin, S. M., J. A. Carton, T. D. Dickey, and J. D. Wiggert (2004), Satellite evidence of hurricane-induced phytoplankton blooms in an oceanic desert, *J. Geophys. Res*., 109, C03043, doi:03010.01029/02003JC001938.

Bailey, S. W. and P. J. Werdell (2006), A multi-sensor approach for the on-orbit validation of ocean color satellite data products. *Remote Sensing of Environment*, 102, 12–23.

Behrenfeld, M. J., J. T. Randerson, C. R McClain, G. C. Feldman, S. O. Los, C. J. Tucker, et al. (2001), Biospheric primary production during an ENSO transition, *Science*, 291, 2594–2597.

Bleck, R., (2002), An oceanic general circulation model framed in hybrid isopycnic-Cartesian coordinate. *Ocean Modell.*, 4, 55–88.

Bleck, R., C. Rooth, D. Hu, and L. T. Smith (1992), Salinity-driven thermocline transients in a wind and thermohaline-forced isopycnic coordinate model of the North Atlantic, J. *Phys. Oceanogr*., 22, 1486–1505.

Brink, K. H. (1989), Observations of the response of thermocline currents to a hurricane, *J. Phys. Oceanogr*., 19, 1017–1022.

Brooks, D. A. (1983), The wake of Hurricane Allen in the western Gulf of Mexico, *J. Phys. Oceanogr*., 13, 117–129.

Chassignet, E. P., H. E. Hurlburt, O. M. Smedstad, G. R. Halliwell, P. J. Hogan, A. J. Wallcraft, R. Baraille, and R. Bleck (2007), The HYCOM (Hybrid Coordinate Ocean Model) data assimilative system, *J. Mar. Syst*., 65, 60– 83.

Chassignet, E., L. Smith, G. Halliwell, and R. Bleck (2003) North Atlantic simulations with the Hybrid Coordinate Ocean Model (HYCOM): Impact of coordinate choice, reference pressure, and thermobaricity, *J. Phys. Oceanogr*., 33, 2504–2526.

Chavez, F. P., P. G. Strutton, G. E. Friederich, R. A. Feely, G. C. Feldman and D. G. Foley, et al. (1999), Biological and chemical response of the Equatorial Pacific Ocean to the 1997 – 98 El Niňo, *Science*, 286, 2128–2131.

Dickey, T. and J. J. Simpson (1983), The sensitivity of upper ocean structure to time varying wind direction, *Geophys. Res. Lett*., 10, 133–136.

Dickey, T., et al. (1998), Upper-ocean temperature response to Hurricane Felix as measured by the Bermuda Testbed Mooring, *Mon. Weather Rev*., 126, 1195–1200.

Fratantoni, P. S., T. N. Lee, G. P. Podesta and F. Muller-Karger (1998), The influence of Loop Current perturbations on the formation and evolution of Tortugas eddies in the southern Straits of Florida, *J. Geophys. Res*., 103(C11): 24759–24799.

Gordon, H. R. (1997), Atmospheric correction of ocean color imagery in the Earth Observing System era, *J. Geophys. Res*., 102, 17,081–017,106.

Gordon, H. R., and M. Wang (1994), Retrieval of water-leaving radiance and aerosol optical thickness over the oceans with SeaWiFS: A preliminary algorithm, *Appl. Opt*., 33, 443–452.

Hale, G. M., and M. R. Querry (1973), Optical constants of water in the 200nm to 200µm wavelength region, Appl. Opt., 12, 555-563.

Hazelworth, J. B. (1968), Water temperature variations resulting from hurricanes, *J. Geophys. Res*., 73, 5105–5123.

Hoge, F. E. and P. E. Lyon (2002), Satellite observation of Chromophoric Dissovled Organic Matter (CDOM) variability in the wake of hurricanes and typhoons, *Geophys. Res. Lett*., 29(19), 1908, doi:10.1029/2002GL015114.

Hooker, S. B., W. E. Esaias, G. C. Feldman, W. W. Gregg and C. R. McClain (1992), An overview of SeaWiFS and Ocean Color, Vol. 1 of SeaWiFS Technical Report Series, In S. B. Hooker & E. R. Firestone (Eds), NASA Tech. Memo, 104566 Greenbelt, Maryland: NASA Goddard Space Flight Center.

Hu, C., and F. E. Muller-Karger (2007), Response of sea surface properties to Hurricane Dennis in the eastern Gulf of Mexico, *Geophys. Res. Lett*., 34, L07606, doi:10.1029/2006GL028935.

Hu, C., et al. (2006), Ocean color reveals phase shift between marine plants and yellow substance, *IEEE Geosci. Remote Sens. Lett.*, 3, 262–266.

IOCCG (2010), Atmospheric correction for remotely-sensed ocean colour products, Wang, M. (ed.), *Reports of the International Ocean-Colour Coordinating Group*, No. 10, IOCCG, Dartmouth, Canada.

Jacob, S. D. and L. K. Shay (2003), The role of mesoscale features on the tropical cyclone–induced mixed layer response: A case study. J. Phys. Oceanogr., 33:649–676.

Jacob, S. D., L. K. Shay, and A. J. Mariano (2000), The 3D oceanic mixed layer response to Hurricane Gilbert, *J. Phys. Oceanogr.*, 30, 1407–1429.

Lavender, S. J., M. H. Pinkerton, G. F. Moore, J. Aiken and D. Blondeau-Patissier (2005), Modification to the atmospheric correction of SeaWiFS ocean color images over turbid waters. Continental Shelf Research, 25, 539 – 555.

Lee, T. N., C. Rooth, E. Williams, M. McGowan, A. F. Szmant and M. E. Clarke (1992), Influence of Florida Current, gyres and wind-driven circulation on transport of larvae and recruitment in the Florida Keys coral reefs, *Cont. Shelf. Res.*, 12: 971–1002.

Lee, T.N., K. Leaman, E. Williams, T. Berger and L. Atkinson (1995), Florida Current meanders and gyre formation in the southern Straits of Florida, *J. Geophys. Res.*, 100(C5): 8607–8620.

Leipper, D. F. (1967), Observed ocean conditions and Hurricane Hilda, 1964, *J. Atmos. Sci.*, 24, 182–196.

Levitus, S. (1982), Climatological atlas of the world ocean, NOAA Prof. Pap. 13, U.S. Govt. Print. Off., Washington, D. C.

Levitus, S., and T. Boyer (1994), World Ocean Atlas 1994 Volume 4: Temperature, U.S. Department of Commerce, Washington, D.C.

Lin, I., W. T. Liu, C-C. Wu, G. T. F. Wong, C. Hu, Z. Chen, W-D. Liang, Y. Yang, and K-K. Liu (2003), New evidence for enhanced ocean primary production triggered by tropical cyclone, *Geophy. Res. Lett.*, 30, 1718, doi:10.1029/2003GL017141.

Liu, X, M. Wang, and W. Shi (2009), A study of a Hurricane Katrina-induced phytoplankton bloom using satellite observations and model simulations, *J. Geophy. Res.*, 114, C03023, doi:10.1029/2008JC004934.

McClain, C. R., G. C. Feldman and S. B. Hooker (2004), An overview of the SeaWiFS project and strategies for producing a climate research quality global ocean bio-optical time series. *Deep Sea Research, Part 2, Topical studies in oceanography*, 51, 5–42.

Miller, W. D., L. W. H. Jr., and J. E. Adolf (2006), Hurricane Isabel generated an unusual fall bloom in Chesapeake Bay, *Geophy. Res. Lett.*, 33, L06612, doi:06610.01029/02005GL025658.

Paluszkiewicz, T., L. P. Atkinson, E. S. Posmentier and C. R. McClain (1983), Observations of a Loop Current Frontal Eddy intrusion onto the West Florida Shelf. *J. Geophys. Res.*, 88: 9639–9652.

Prasad, T. G., and P. J. Hogan (2007), Upper-ocean response to Hurricane Ivan in a $1/25^{o}$ nested Gulf of Mexico HYCOM, J. Geophys. Res., 112, C04013, doi:10.1029/2006JC003695.

Price, J. F. (1981), Upper ocean response to a hurricane, *J. Phys. Oceanogr.*, 11, 153–175.

Price, J. F., T. B. Sanford, and G. Z. Forristall (1994), Forced stage response to a moving hurricane, *J. Phys. Oceanogr.*, 24, 233–260.

Romanou, A., E. P. Chassignet, and W. Sturges (2004), Gulf of Mexico circulation within a high-resolution numerical simulation of the North Atlantic Ocean, *J. Geophys. Res.*, 109, C01003, doi:10.1029/2003JC001770.

Salomonson, V. V., W. L. Barnes, P. W. Maymon, H. E. Montgomery and H. Ostrow (1989), MODIS: Advanced facility instrument for studies of the Earth as a system, *IEEE Transactions on Geoscience and Remote Sensing*, 27, 145–152.

Sanford, T. B., P. G. Black, J. R. Haustein, J. W. Feeney, G. Z. Forristall, and J. F. Price (1987), Ocean response to a hurricane, part I: Observations, *J. Phys. Oceanogr.*, 17, 2065–2083.

Shay, L. K., A. J. Mariano, S. D. Jacob, and E. H. Ryan (1998), Mean and near-inertial ocean current response to Hurricane Gilbert, *J. Phys. Oceanogr.*, 28, 858–889.

Shay, L. K., and R. L. Elsberry (1987), Near-inertial ocean current response to Hurricane Frederic, *J. Phys. Oceanogr.*, 17, 1249–1269.

Shay, L. K., R. L. Elsberry, and P. G. Black (1989), Vertical structure of the ocean current response to a hurricane, *J. Phys. Oceanogr.*, 19, 649–669.

Siegel, D. A., M. Wang, S. Maritorena, and W. Robinson (2000), Atmospheric correction of satellite ocean color imagery: the black pixel assumption, *Appl. Opt.*, 39, 3582–3591.

Shi, W., and M. Wang (2007), Observations of a Hurricane Katrina induced phytoplankton bloom in the Gulf of Mexico, *Geophys. Res. Lett.*, 34, L11607, doi:10.1029/2007GL029724.

Shi, W., and M. Wang (2009), An assessment of the black ocean pixel assumption for MODIS SWIR bands, *Remote Sens. Environ.*, 113, 1587–1597.

Stramma, L., P. Cornillon, and J. F. Price (1986), Satellite observations ofsea surface cooling by hurricanes, *J. Geophys. Res.*, 91, 5031–5035.

Vukovich, F. M. (1988), On the formation of elongated cold perturbations off the Dry Tortugas, *J. Phys. Oceanogr.*, 18: 1051–1059.

Walker, N. D., R. R. Leben, and S. Balasubramanian (2005), Hurricane-forced upwelling and chlorophyll a enhancement within cold-core cyclones in the Gulf of Mexico, *Geophy. Res.* Lett., 32, L18610, doi:18610.11029/12005GL023716.

Wang, M., and W. Shi (2005), Estimation of ocean contribution at the MODIS near-infrared wavelengths along the east coast of the U.S.: Two case studies, *Geophy. Res. Lett.*, 32, L13606, doi:13610.11029/12005GL022917.

Wang, M. (2007), Remote sensing of the ocean contributions from ultraviolet to near-infrared using the shortwave infrared bands: simulations, *Appl. Opt.*, 46, 1535–1547.

Wang, M., J. Tang, and W. Shi (2007), MODIS-derived ocean color products along the China east coastal region, *Geophys. Res. Lett.*, 34, L06611, doi:10.1029/2006GL028599.

Wang, M., S. Son, and W. Shi (2009), Evaluation of MODIS SWIR and NIR-SWIR atmospheric correction algorithms using SeaBASS data, *Remote Sens. Environ.*, 113, 635–644.

Wentz, F. J., C. Gentemann, D. Smith, and D. Chelton (2000), Satellite measurements of sea surface temperature through clouds, Science, 288, 847-850.

Wren, P. A., and L. A. Leonard (2005), Sediment transport on the midcontinental shelf in Onslow Bay, North Carolina during Hurricane Isabel, *Estuarine Coastal Shelf Sci.*, 63, 43–56.

Xie, L., X. Liu, and L.J. Pietrafesa (2007), Effect of Bathymetric Curvature on Gulf Stream Instability in the Vicinity of the Charleston Bump. *J. Phys. Oceanogr.*, 37, 452–475.

Zedler, S. E., T. D. Dickey, S. C. Doney, J. F. Price, X. Yu, and G. L. Mellor (2002), Analyses and simulations of the upper ocean's response to Hurricane Felix at the Bermuda Testbed Mooring site: August 13–23, 1995, *J. Geophys. Res.*, 107, 3232, doi:10.1029/2001JC000969.

Recent Hurricane Research - Climate, Dynamics, and Societal Impacts

Edited by Prof. Anthony Lupo

ISBN 978-953-307-238-8
Hard cover, 616 pages
Publisher InTech
Published online 19, April, 2011
Published in print edition April, 2011

This book represents recent research on tropical cyclones and their impact, and a wide range of topics are covered. An updated global climatology is presented, including the global occurrence of tropical cyclones and the terrestrial factors that may contribute to the variability and long-term trends in their occurrence. Research also examines long term trends in tropical cyclone occurrences and intensity as related to solar activity, while other research discusses the impact climate change may have on these storms. The dynamics and structure of tropical cyclones are studied, with traditional diagnostics employed to examine these as well as more modern approaches in examining their thermodynamics. The book aptly demonstrates how new research into short-range forecasting of tropical cyclone tracks and intensities using satellite information has led to significant improvements. In looking at societal and ecological risks, and damage assessment, authors investigate the use of technology for anticipating, and later evaluating, the amount of damage that is done to human society, watersheds, and forests by land-falling storms. The economic and ecological vulnerability of coastal regions are also studied and are supported by case studies which examine the potential hazards related to the evacuation of populated areas, including medical facilities. These studies provide decision makers with a potential basis for developing improved evacuation techniques.

How to reference

In order to correctly reference this scholarly work, feel free to copy and paste the following:

Menghua Wang, Xiaoming Liu, and Wei Shi (2011). Hurricane-Induced Phytoplankton Blooms: Satellite Observations and Numerical Model Simulations, Recent Hurricane Research - Climate, Dynamics, and Societal Impacts, Prof. Anthony Lupo (Ed.), ISBN: 978-953-307-238-8, InTech, Available from: http://www.intechopen.com/books/recent-hurricane-research-climate-dynamics-and-societal-impacts/hurricane-induced-phytoplankton-blooms-satellite-observations-and-numerical-model-simulations

INTECH
open science | open minds

InTech Europe
University Campus STeP Ri
Slavka Krautzeka 83/A
51000 Rijeka, Croatia
Phone: +385 (51) 770 447
Fax: +385 (51) 686 166

InTech China
Unit 405, Office Block, Hotel Equatorial Shanghai
No.65, Yan An Road (West), Shanghai, 200040, China
中国上海市延安西路65号上海国际贵都大饭店办公楼405单元
Phone: +86-21-62489820
Fax: +86-21-62489821

INTECH